Neuron
Article

Distributed Network Actions by Nicotine Increase the Threshold for Spike-Timing-Dependent Plasticity in Prefrontal Cortex

Jonathan J. Couey,[1] Rhiannon M. Meredith,[1] Sabine Spijker,[2] Rogier B. Poorthuis,[1] August B. Smit,[2] Arjen B. Brussaard,[1] and Huibert D. Mansvelder[1,*]
[1] Department of Experimental Neurophysiology
[2] Department of Molecular and Cellular Neurobiology
Center for Neurogenomics and Cognitive Research, Vrije Universiteit Amsterdam, 1081 HV, Amsterdam, The Netherlands
*Correspondence: huib@cncr.vu.nl
DOI 10.1016/j.neuron.2007.03.006

SUMMARY

Nicotine enhances attention and working memory by activating nicotinic acetylcholine receptors (nAChRs). The prefrontal cortex (PFC) is critical for these cognitive functions and is also rich in nAChR expression. Specific cellular and synaptic mechanisms underlying nicotine's effects on cognition remain elusive. Here we show that nicotine exposure increases the threshold for synaptic spike-timing-dependent potentiation (STDP) in layer V pyramidal neurons of the mouse PFC. During coincident presynaptic and postsynaptic activity, nicotine reduces dendritic calcium signals associated with action potential propagation by enhancing GABAergic transmission. This results from a series of presynaptic actions involving different PFC interneurons and multiple nAChR subtypes. Pharmacological block of nAChRs or $GABA_A$ receptors prevented nicotine's actions and restored STDP, as did increasing dendritic calcium signals with stronger postsynaptic activity. Thus, by activating nAChRs distributed throughout the PFC neuronal network, nicotine affects PFC information processing and storage by increasing the amount of postsynaptic activity necessary to induce STDP.

INTRODUCTION

Nicotine is the addictive ingredient in tobacco that drives people to dependence, but it has also been shown to improve cognitive function in humans and laboratory animals (Levin et al., 2005; Levin, 1992; Mansvelder et al., 2006; Newhouse et al., 2004b). In smokers and patients suffering from a variety of neuropsychiatric disorders, nicotinic agonists act beneficially on several aspects of cognition, including working memory, attention, learning, and memory. In fact, nicotinic treatments are being developed as therapy for cognitive dysfunction in disorders such as Alzheimer's disease, Parkinson's disease, schizophrenia, and ADHD (Levin et al., 2005; Newhouse et al., 2004a, 2004b; Picciotto and Zoli, 2002). In contrast, in normal nonsmokers, nicotine tends to have deleterious effects on cognitive performance (Newhouse et al., 2004b). Although it is likely that many brain areas contribute to the nicotinic effects on cognition, based on animal studies nicotinic acetylcholine receptors (nAChRs) in the prefrontal cortex (PFC) mediate the effects on attention and working memory performance (Granon et al., 1995; Levin, 1992; Muir et al., 1995). The rodent medial PFC is considered to be functionally homologous to the primate dorsolateral PFC and has been shown to be involved in attention and working memory (Dalley et al., 2004; Groenewegen and Uylings, 2000). Despite this understanding of nicotinic effects on working memory and attention performance, very little is known of the cellular and synaptic mechanisms involved in the enhancement of these functions.

Excitatory glutamatergic synapses in the PFC are plastic, and changes in synaptic strength occur in the rodent PFC during working-memory-related tasks (Jay et al., 1995; Laroche et al., 1990, 2000). Changes in strength of cortical synapses are thought to occur depending on the precise timing of pre- and postsynaptic activity, a process known as spike-timing-dependent plasticity (Bi and Poo, 1998; Magee and Johnston, 1997; Markram et al., 1997). The relative timing of pre- and postsynaptic activity results in specific postsynaptic changes in calcium concentration that determine whether synaptic strength will increase or decrease (Koester and Sakmann, 1998; Sjostrom and Nelson, 2002). nAChRs are ligand-gated cation channels that—depending on their subcellular location—can alter presynaptic release of neurotransmitters as well as dendritic membrane potential (MacDermott et al., 1999; McGehee and Role, 1995). These nicotine-induced cellular and synaptic alterations have been shown to affect the induction of long-term changes in synaptic strength in the ventral tegmental area (VTA) and hippocampus (Ge and Dani, 2005; Ji et al., 2001; Mansvelder and McGehee, 2000). These and other studies highlight that, in order to

understand nicotinic modulation of information processing in a particular brain area, one needs to understand how nicotine affects the different cell types in the neuronal network. More specifically, nicotinic modulation of a neuronal network depends on (1) the types of neurons in the network that express nAChRs; (2) the types of nAChRs expressed; and (3) the subcellular location of these nAChRs (Alkondon and Albuquerque, 2004; Ji et al., 2001; MacDermott et al., 1999; Mansvelder and McGehee, 2002; McGehee and Role, 1996; Wonnacott et al., 2005). To our knowledge, none of these aspects have been addressed in the PFC (Gioanni et al., 1999; Lambe et al., 2003; Mansvelder et al., 2006; Vidal and Changeux, 1989, 1993).

Therefore, to understand the synaptic and cellular mechanisms underlying nicotinic enhancement of PFC-based cognition, we investigated how nicotinic modulation of the PFC neuronal network affects spike-timing-dependent potentiation (STDP). We find that nicotine increases the threshold for induction of STDP in pyramidal neurons. This effect is caused by a reduction of dendritic calcium signaling in these neurons as a result of nicotine-induced augmentation of GABAergic inhibition. Our study also demonstrates that both specific classes of PFC interneurons express nAChRs, and that specific inputs to these cell types in the medial PFC neuronal circuitry are modulated by nAChR stimulation. By affecting different parts of the PFC neuronal network through activating different nAChR types, nicotine raises the threshold for the induction of STDP in PFC output neurons.

RESULTS

Nicotine Blocks Spike-Timing-Dependent Potentiation of Glutamatergic Transmission

Since nicotine alters cognitive performance of rodents in behavioral tasks that involve PFC function (Granon et al., 1995), and since changes in excitatory synapse strength occur during such tasks (Jay et al., 1995; Laroche et al., 1990, 2000), we asked whether nicotine alters synaptic plasticity in medial PFC. To test this, we made whole-cell recordings from layer V pyramidal neurons and stimulated glutamatergic inputs by extracellular stimulation (Figure 1A). Pyramidal neurons were identified based on morphological appearance in the differential interference contrast (DIC) image and action potential profile in response to step depolarizations (Figure 1B). To induce STDP, extracellular stimulation of presynaptic glutamatergic input was paired with a single postsynaptic action potential evoked by somatic current injection (Figure 1A, inset). Repeated pairing of the EPSP with a single postsynaptic action potential (5 ms after start of EPSP, 50× at 0.1 Hz) resulted in a lasting increase of both EPSP amplitude and slope (increase in slope: 133.3% ± 19.7%; Figures 1D and 1H).

When nicotine (10 μM) was applied briefly during the start of the pairing period, glutamatergic synaptic strength failed to increase (Figures 1E and 1H). Instead, nicotine induced a small and significant reduction in synaptic weight to 87.0% ± 10.3% of control after induction (Figures 1H and 1I). During cigarette smoking, blood levels of nicotine rapidly increase to 300–500 nM (Henningfield et al., 1993). Application of 300 nM nicotine during pairing of pre- and postsynaptic activity also prevented the increase of synaptic weight (n = 5, Figures 1F and 1H). Similarly to 10 μM nicotine, application of 300 nM nicotine resulted in a tendency toward a reduction of synaptic strength (Figures 1H and 1I), but this did not reach significance. The broad-spectrum nicotinic receptor antagonist mecamylamine (MEC, 1 μM) prevented the effect of nicotine (Figures 1G and 1H). In the presence of both MEC and nicotine, the pairing of EPSP and postsynaptic action potential induced a synaptic gain that was indistinguishable from that in control conditions (n = 8, Figures 1H and 1I). Thus, activation of nicotinic receptors in medial PFC prevents STDP of inputs (evoked in layer II/III) to layer V pyramidal cells and induces LTD instead.

Direct Nicotinic Actions on Evoked Glutamatergic Transmission

The most straightforward mechanism by which nicotine alters synaptic plasticity is through activation of either postsynaptic nAChRs or presynaptic nAChRs on the glutamatergic terminals. In other brain areas, activation of nAChRs located on presynaptic glutamatergic terminals increases release of glutamate directly (Gray et al., 1996; McGehee et al., 1995). In VTA, activation of these presynaptic nAChRs can induce LTP (Mansvelder and McGehee, 2000). In PFC, nicotine also augments spontaneous excitatory glutamatergic synaptic transmission to layer V pyramidal neurons by activating presynaptic nAChRs (Gioanni et al., 1999; Lambe et al., 2003; Vidal and Changeux, 1989, 1993). This effect depends on action potential firing, indicating that nAChRs are located away from the presynaptic terminals. In our hands, nicotine also induced an increase in frequency and amplitude of spontaneous EPSCs (Figures 2A and 2B). The EPSCs disappeared in the presence of the AMPA receptor blocker DNQX (10 μM, n = 4; see Figures S1A and S1B in the Supplemental Data). Because nicotine's effect on spontaneous release of glutamate was opposite to its effect on STDP, we next tested if nicotine affected evoked glutamatergic transmission by applying stimulation either in layer II/III or in layer V while recording from layer V pyramidal neurons (Figure 2D). Evoked EPSCs resulting from stimulation of layer II/III or layer V were not increased in amplitude by nicotine (Figures 2E and 2F). Instead, evoked EPSC amplitude showed a small transient reduction that hardly outlasted the nicotine application (Figure 2F). Furthermore, puffing nicotine directly onto pyramidal neurons did not elicit an inward current (n = 15, Figure 2C), suggesting that as in other neocortical areas, PFC layer V pyramidal neurons do not express functional nAChRs. These data demonstrate that activation of presynaptic glutamatergic inputs or postsynaptic nAChRs on pyramidal neurons cannot explain the effect of nicotine on STDP in PFC.

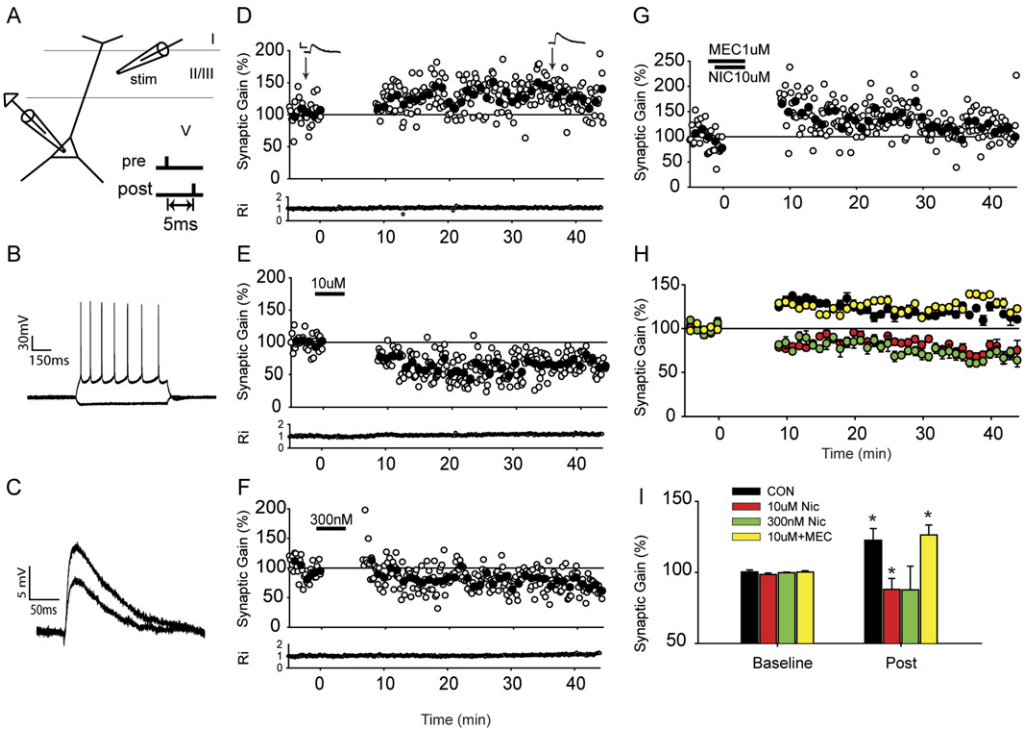

Figure 1. Spike-Timing-Dependent Potentiation In Layer V Pyramidal Cells of the Mouse Prefrontal Cortex

(A) Graphic scheme of experimental setup depicting placement of extracellular stimulating electrode and timing of STDP induction protocol (inset).

(B) Representative current-clamp traces from a layer V pyramidal cell (injection of −100 and +50 pA).

(C) Example EPSPs recorded before (smaller) and after (larger) STDP induction.

(D–G) Example experiments showing spike-timing-dependent potentiation (STDP) in a layer V pyramidal cell for (D) control, (E) 10 μM nicotine, (F) 300 nM nicotine, and (G) 10 μM nicotine and 1 μM mecamylamine (MEC). Duration of applications is indicated by the bars above the graphs. In (G), synaptic gain at 35–45 min after induction is significantly above baseline ($p < 0.05$), in line with the average shown in (H). Inset traces in (D) show example EPSPs. Scale bars same as in (C).

(H) Average temporal plot comparing change in EPSP slope in control (black circles, n = 6), nicotine (10 μM: red circles, n = 7; 300 nM: green circles, n = 5) and nicotine with MEC (yellow circles, n = 8).

(I) Bar graph summarizing STDP in control, nicotine, and MEC. *$p < 0.05$.

Error bars = SEM.

Blocking $GABA_A$ Receptors, but Not $GABA_B$ Receptors, Strongly Reduces Nicotine's Impact on STDP

An alternative mechanism by which nicotine could affect STDP in PFC is through activation of nAChRs, on either the terminals or somata of inhibitory GABAergic neurons. Indeed, in many cortical and subcortical brain areas, nicotine affects not only glutamatergic but also GABAergic synaptic transmission (Alkondon and Albuquerque, 2004; Dani and Harris, 2005; Mansvelder et al., 2002, 2006; Metherate, 2004). In hippocampus, timed activation of GABAergic interneurons by nicotine diminishes or prevents long-term potentiation (LTP) in pyramidal neurons (Ji et al., 2001). To investigate whether GABAergic transmission mediates nicotine's effect on STDP, we tested how the $GABA_A$ receptor blocker gabazine and the $GABA_B$ receptor blocker CGP-54626 affected nicotine's impact on STDP. In the presence of gabazine (0.25–1 μM), the reduction of STDP by nicotine was much less than with nicotine alone (n = 8, $p < 0.05$; Figures 3A and 3C). In contrast, CGP-54626 (5 μM) did not affect the block of potentiation by nicotine (n = 5, Figures 3B and 3C). These results indicate that increased GABAergic signaling through $GABA_A$ receptors mediates nicotine's block of STDP in PFC.

Nicotine Enhances Inhibitory GABAergic Transmission to Pyramidal Neurons

To assess the extent to which nicotine affects inhibitory GABAergic transmission received by layer V pyramidal neurons, inhibitory postsynaptic currents were evoked by stimulating layer II/III while recording from layer V pyramidal neurons. The amplitude of evoked IPSCs was transiently enhanced by nicotine (Figures 4A and 4B). On average nicotine increased the GABAergic synaptic strength by 141% ± 11%, which subsided when nicotine was washed out (Figure 4B). Nicotine also affected spontaneous inhibitory synaptic transmission. Both frequency and amplitude of spontaneous IPSCs strongly increased in all cells tested when nicotine (10 μM) was bath-applied (n = 7, Figures 4C–4E). IPSC frequency was increased to

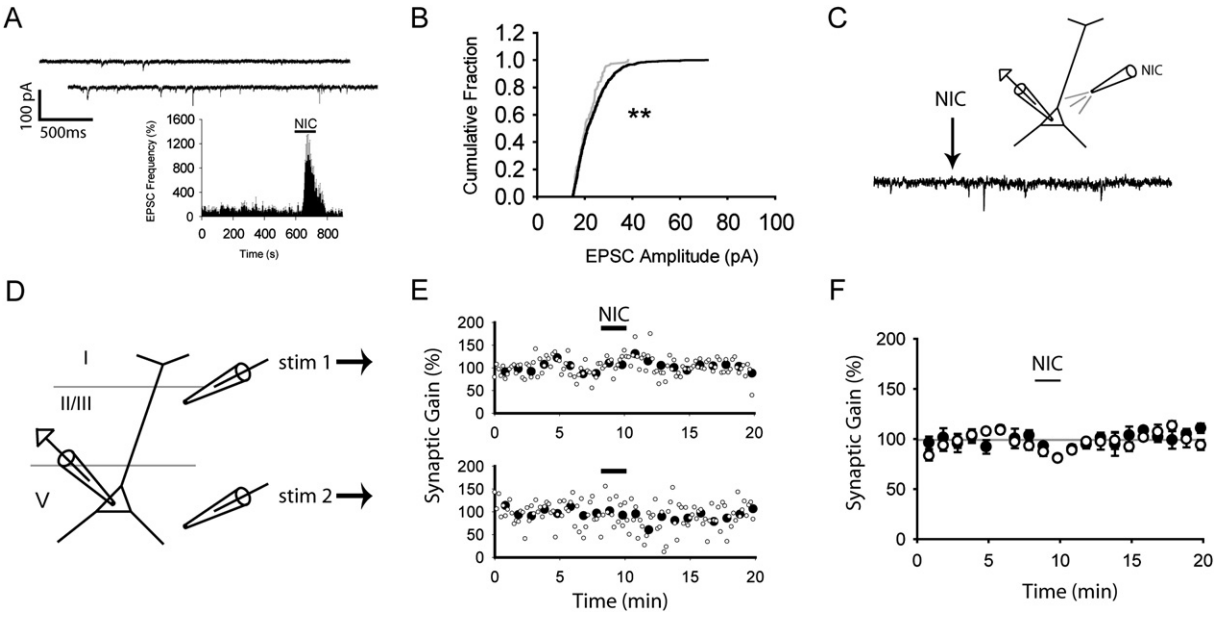

Figure 2. Glutamatergic Inputs to Layer V Pyramidal Cells

(A) Example trace with spontaneous EPSCs recorded in a layer V pyramidal cell. Top trace: control; lower trace: in the presence of 10 μM nicotine. Scale bar, 100 pA, 500 ms. (Inset below) Frequency histogram for spontaneous EPSCs (n = 6).

(B) Cumulative EPSC amplitude distribution before (gray) and after (black) nicotine application. Data is taken from experiment shown in (A).

(C) Voltage-clamp trace from a layer V pyramidal cell where nicotine was locally applied at the arrow and no current was observed (n = 14). Inset above shows experimental setup.

(D) Experimental setup for (E).

(E) Normalized amplitude of evoked EPSPs (gray circles) and mean amplitude per minute (black circles) recorded from the two stimulation locations depicted in (D).

(F) Average plot of evoked EPSP experiments from layer II/III (white circles) and layer V (black circles) (n = 6).

Error bars = SEM.

246% ± 72%. Low nicotine concentrations (300 nM) also augmented spontaneous IPSC frequency by 131.5% ± 3% (n = 5, Figure 4F). IPSC amplitude distribution was increased in all cells tested. Cumulative amplitude distributions showed that nicotine had a strong effect on larger-amplitude synaptic currents (Figure 4E). IPSCs disappeared when bicuculline (10 μM) was applied (n = 3, Figures S1C and S1D), and nicotine's effect was blocked by TTX (n = 3, Figure S2B). These experiments show that in addition to augmenting excitatory synaptic transmission to PFC pyramidal neurons, inhibitory GABAergic transmission is also enhanced by nicotine.

As an initial pharmacological characterization of the nAChR subtypes involved in augmenting spontaneous GABAergic transmission in PFC pyramidal neurons, we tested the effect of nicotine in the presence of MEC and methyllycaconitine (MLA), which is more selective for α7-containing nAChRs. In the presence of MLA (10 nM), nicotine still increased the frequency of spontaneous IPSCs, but not in all cells tested. In three out of four cells, nicotine increased the IPSC frequency to 294% ± 18% (Figure 4G). The IPSC amplitude distribution was also shifted to larger amplitudes in three out of four cells (Figure S2A). This suggests that MLA-sensitive nAChRs do contribute to the effect of nicotine on spontaneous IPSCs. In the presence of MEC (1 μM), nicotine application did not affect the frequency of spontaneous IPSCs in five out of seven cells. Also, the effect of nicotine on amplitude distribution was blocked in five out of seven cells (Figures 4H and 4I). Nicotine most likely activates multiple types of nAChRs to increase both frequency and amplitude of spontaneous IPSCs and augment inhibition of PFC pyramidal neurons.

Nicotine Excites Different Types of Interneurons through Multiple Mechanisms

To delineate which types of interneurons express functional nAChRs, we targeted different classes of interneurons for whole-cell recording. In rat PFC several types of pyramidal neurons and interneurons have been described based on electrophysiological profile, morphology, and expression of calcium binding proteins (Gabbott et al., 1997; Gulledge et al., 2007; Kawaguchi, 1993; Kawaguchi and Kondo, 2002; Kawaguchi and Kubota, 1997; Yang et al., 1996). As far as we are aware, a characterization of interneurons in mouse medial PFC has not been described in the literature thus far, and we identified three different classes of interneurons based on action potential

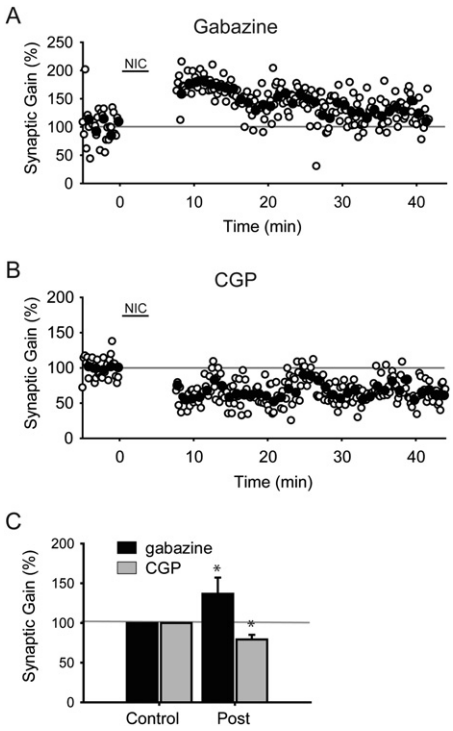

Figure 3. Effect of GABAergic Inhibition on Spike-Timing-Dependent LTP

(A) Example trace of STDP in a layer V pyramidal neuron in the presence of 10 μM nicotine and 1 μM of the $GABA_A$ antagonist gabazine.
(B) Example trace of blocked potentiation in the presence of 10 μM nicotine and 5 μM of the $GABA_B$ receptor blocker CGP-54626.
(C) Summary bar graph. *$p < 0.05$.
Error bars = SEM.

firing profile in response to current steps (Figures 5A–5C). Their morphological appearance was clearly distinct from the typical layer V pyramidal neuron morphology (Figures 5A–5C, insets).

The first type of interneuron had the typical characteristics of fast-spiking (FS) interneurons in other cortical areas (Kawaguchi and Kondo, 2002). They were multipolar with round cell bodies. In response to step current injections, they showed nonadapting, tonic firing behavior with a firing frequency that was proportional to the amount of depolarizing current injection (Figure 5A). Local puffs (100 ms) of nicotine to the cell body region of this type of interneuron did not elicit inward currents in any of the cells tested (n = 24; Figures 5D, 5G, and 5H).

The action potential profile of a different type of interneuron showed slight adaptation in response to step current injections (Figure 5B). These cells had a multipolar appearance similar to that of FS cells. These cells were named regular spiking nonpyramidal neurons (RSNP). In response to local application of nicotine, a fast inward current of 12 ± 6 pA was activated in about half of the RSNP neurons (n = 60; Figures 5E, 5G, and 5H).

The third type of interneuron showed strong adaptation of firing frequency in response to step depolarizations and had a lower threshold for firing (Figure 5C). In many cases, these cells fired rebound spikes after a step hyperpolarization. Therefore, these cells were named low-threshold spiking (LTS) cells. As FS cells, LTS cells had a bipolar appearance or showed, in addition to smaller multipolar dendrites, one dendrite of larger diameter that pointed toward layer VI. These cells often also showed a limited number of dendritic spines. Upon application of nicotine to their somatic region, a large inward current of 28 ± 10 pA was activated in all cells tested, with a faster rise time than the nicotine-induced current in RSNP cells (n = 10; Figures 5F, 5G, and 5H). The amplitude of nicotine-induced currents was largest in these cells, and nearly double the amplitude of nicotine-induced currents in RSNP cells (Figure 5H).

During and after pressure application of nicotine, noise levels in recordings from RSNP and LTS cells increased. In RSNP cells (Figure 5E), the noise at the peak of the nicotine-induced current was increased from 29.9 ± 0.026 pA to 52.1 ± 16.0 pA and diminished in 4 s to 42.4 ± 20.9 pA. In contrast, in LTS cells (Figure 5F), the noise at the peak of the nicotine-induced current was not larger than at baseline (29.8 ± 0.018 pA versus 29.7 ± 0.19 pA), but steadily increased during 4 s to 49.4 ± 1.54 pA at the end of the trace. Most likely, open-channel noise from nAChRs contributes to the noise in both, but nicotine might also activate synaptic currents in these neurons.

Different Types of Interneurons Differentially Express mRNA for nAChRs

To test which nAChR subunits were expressed by the different types of interneurons, we determined the presence of mRNAs for the most abundant nAChRs in the brain, α4, β2, and α7, using single-cell PCR (Cauli et al., 2000; Liss, 2002). After establishing the whole-cell configuration in the PFC slice and applying step current injections to obtain the action potential profile of the interneuron, the cell contents were aspirated into the recording pipette and real-time PCR was performed on the tip contents (Table 1). GAD2 mRNA, encoding the glutamic acid decarboxylase enzyme GAD65, was abundantly detected in all three interneuron types, suggesting that these cells synthesize the neurotransmitter GABA. In addition, expression of genes encoding different calcium binding proteins and peptides was detected in these cells. RSNP cells abundantly expressed calbindin (CB) and cholecystokinin (CCK), but to a lesser extend somatostatin (SOM). In contrast, a much smaller proportion of FS cells expressed CCK, whereas the majority of FS cells expressed CB and SOM. LTS cells expressed CB, CCK, and SOM to a similar degree (Table 1). nAChR mRNA expression patterns were in line with the responses of interneurons to nicotine puffs to the soma. FS cells did not show inward currents upon nicotine application (Figure 5), and hardly any FS cells showed expression for nAChR mRNA. In

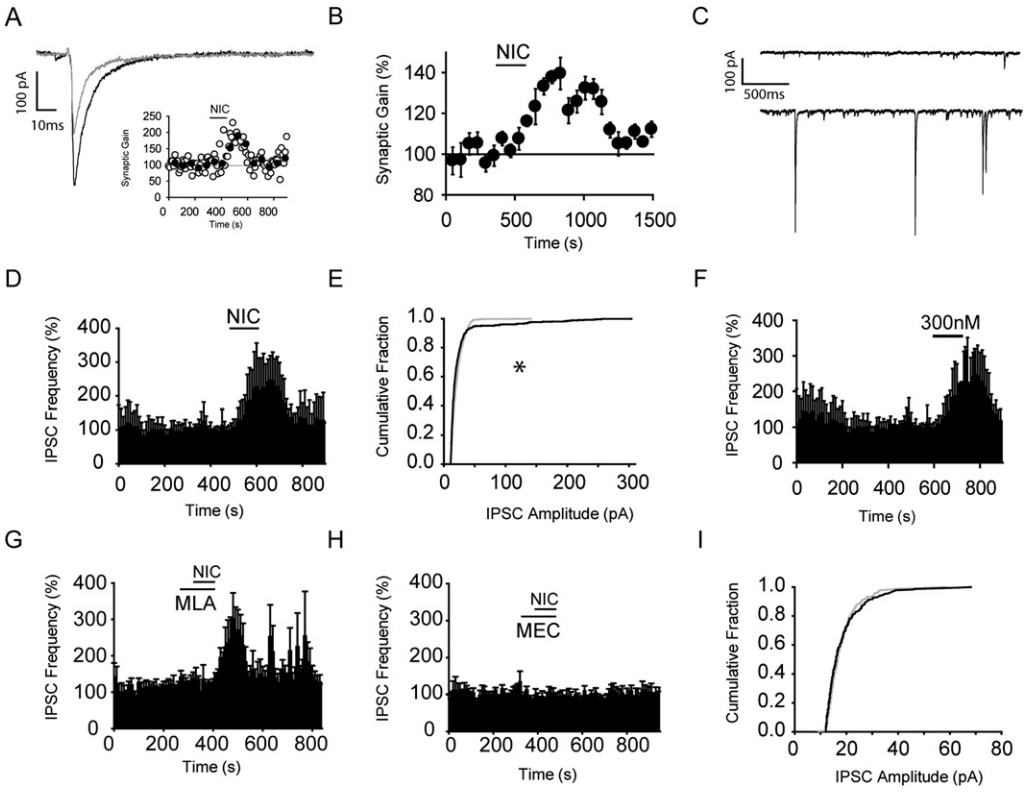

Figure 4. GABAergic Transmission to Layer V Pyramidal Cells

(A) Example evoked IPSCs before (gray trace) and after (black trace) nicotine application. (Inset) Temporal plot of normalized amplitude (white circles) and mean per minute (black circles) from a single experiment.

(B) Summary of evoked IPSC experiments (n = 6).

(C) Example spontaneous IPSCs recorded from a layer V pyramidal cell in the absence (top trace) and presence(bottom trace) of 10 μM nicotine.

(D) Average IPSC frequency histogram (n = 7).

(E) Cumulative IPSC amplitude distribution from experiment shown in (D) ($p < 0.001$).

(F) Average IPSC frequency histogram with 300 nM nicotine application (n = 5).

(G) Average IPSC frequency histogram (n = 4). Duration of MLA and nicotine application is indicated by bars above graph.

(H) Average IPSC frequency histogram with the application of MEC and nicotine (n = 7).

(I) Cumulative IPSC amplitude distribution from a single MEC/nicotine experiment ($p = 0.3$).

Error bars = SEM.

contrast, LTS and RSNP cells both showed functional responses to nicotine application to the soma (Figure 5), and in both cell types mRNA encoding nAChR subunits was found (Table 1). The largest number of LTS and RSNP cells expressed α4 subunits, but β2 and α7 mRNA was also found in these cell types. These data are also in line with the finding that the augmentation of spontaneous IPSCs by nicotine has a mixed pharmacological profile (Figures 4G and 4H and Figure S2).

Excitatory Inputs to Different Types of Interneurons Are Differentially Affected by Nicotine

We have shown that the mouse medial PFC harbors at least three classes of interneurons that show similar functional and morphological properties to interneurons found in other cortical areas but differ in functional nAChR expression. FS cells do not express nAChRs somatically, whereas RSNP and LTS cells express functional nAChRs and contain mRNA for α4, β2, and α7 subunits. These cell types are directly depolarized by nAChR activation expressed on their cell bodies or proximal dendrites, and LTS cells could even be made to spike when nicotine was applied in current clamp (Figure 5F, inset). These somatic nAChRs could account for the increase in IPSC frequency and amplitude observed in recordings from pyramidal neurons after application of nicotine (Figure 4). However, as excitatory inputs to pyramidal neurons are modulated by nicotine, excitatory inputs to interneurons could also be modulated by nAChR activation, which would also contribute to increased GABAergic activity by nicotine. Therefore, we monitored spontaneous EPSCs in whole-cell recordings from the three interneuron types.

Nicotine differentially modulated spontaneous excitatory transmission in medial PFC interneurons. Spontaneous EPSCs in FS cells showed a substantial increase in both EPSC frequency and amplitude (Figures 6A–6C).

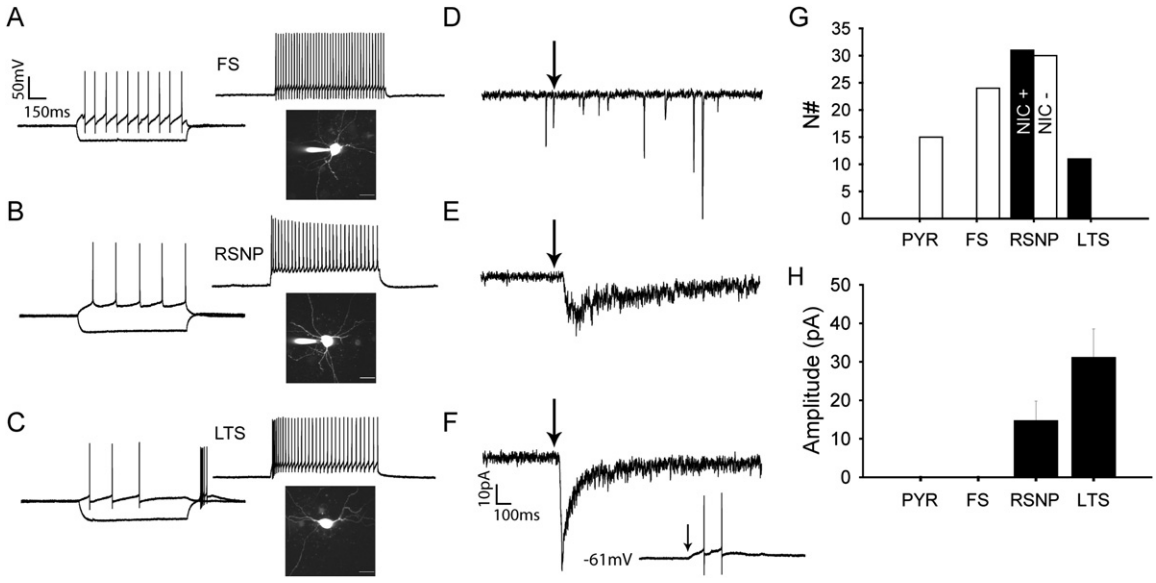

Figure 5. Local Application of Nicotine onto PFC Interneurons

(A–C) Example current-clamp recordings and morphology of Alexa-filled cells illustrating the three basic interneurons observed in mouse PFC: fast-spiking cells (FS), regular spiking nonpyramidal cells (RSNP), and low-threshold spiking cells (LTS).

(D–F) Example voltage-clamp traces in each of the three cell types depicted in (A) where nicotine was locally applied to the soma (100 ms pressure ejection at arrow). (F, Inset) Current-clamp recording showing that single somatic application of nicotine onto LTS cells can induce spiking.

(G) Histogram comparing the number of cells in each cell class that were positive (black) and negative (white) for nicotinic currents.

(H) Histogram showing average current observed in positive cells from (G).

EPSC frequency increased by 360% ± 144%, and the cumulative distribution of EPSC amplitudes showed that significantly more EPSCs with amplitudes above 25 pA were recruited by nicotine (Figures 6B and 6C). This effect was blocked by MEC (n = 10, Figure S3A) and TTX (n = 6, Figure S3B). In contrast, spontaneous EPSCs recorded in RSNP cells were negatively modulated by nicotine. EPSC frequency, but not amplitude, was significantly lower in the presence of bath-applied nicotine (Figures 6D–6F). The number and amplitude of spontaneous EPSCs recorded in LTS cells were increased by nicotine. Both EPSC frequency and amplitude were increased significantly by nicotine application (Figures 6G–6I).

Thus, although FS cells do not seem to express functional nAChRs, their excitatory glutamatergic inputs are increased by nicotine, and they will thus receive an increased excitatory drive in the presence of nicotine. Nicotine will directly depolarize RSNP cells by activating nAChRs on the cell body, but excitatory inputs to these cells are not decreased in amplitude. LTS cells experience an increased excitatory drive from both activated nAChRs on the cell body and an increased glutamatergic input. Our data suggest that all interneuron classes we encountered potentially contribute to the increased inhibition observed in pyramidal neurons in the presence of nicotine.

Dendritic Calcium Signaling Is Reduced by Nicotine during Induction of STDP

Inhibitory GABAergic synaptic transmission controls dendritic action potential propagation in pyramidal neurons. In the hippocampus, IPSPs modulate action potential propagation and calcium signaling, and during development, increased GABAergic inhibition changes the rules for STDP in these neurons (Meredith et al., 2003; Tsubokawa and Ross, 1996). Postsynaptic calcium transients provide an associative link between synapse activation, postsynaptic cell firing, and synaptic plasticity (Koester and Sakmann, 1998; Malenka et al., 1988). Since IPSCs in PFC

Table 1. Percentage of Cells Positive for Neuropeptides and nAChR Subunits

	GAD2	CB	CCK	SOM	α4	β2	α7
FS (12)	++	++	−	+	−−	−	−−
LTS (9)	++	+	+	+	++	+/−	+/−
RSNP (27)	++	++	++	−−	++	+	+/−

Cells (% positive) for neuropeptides (GAD2, CB, CCK, and SOM) and nAChR subunits (α4, β2, and α7): 0%–10%, −− ; 10%–20%, − ; 20%–30%, +/− ; 30%–40%, + ; 40%–50+%, ++. The number of cells assessed is indicated parenthetically.

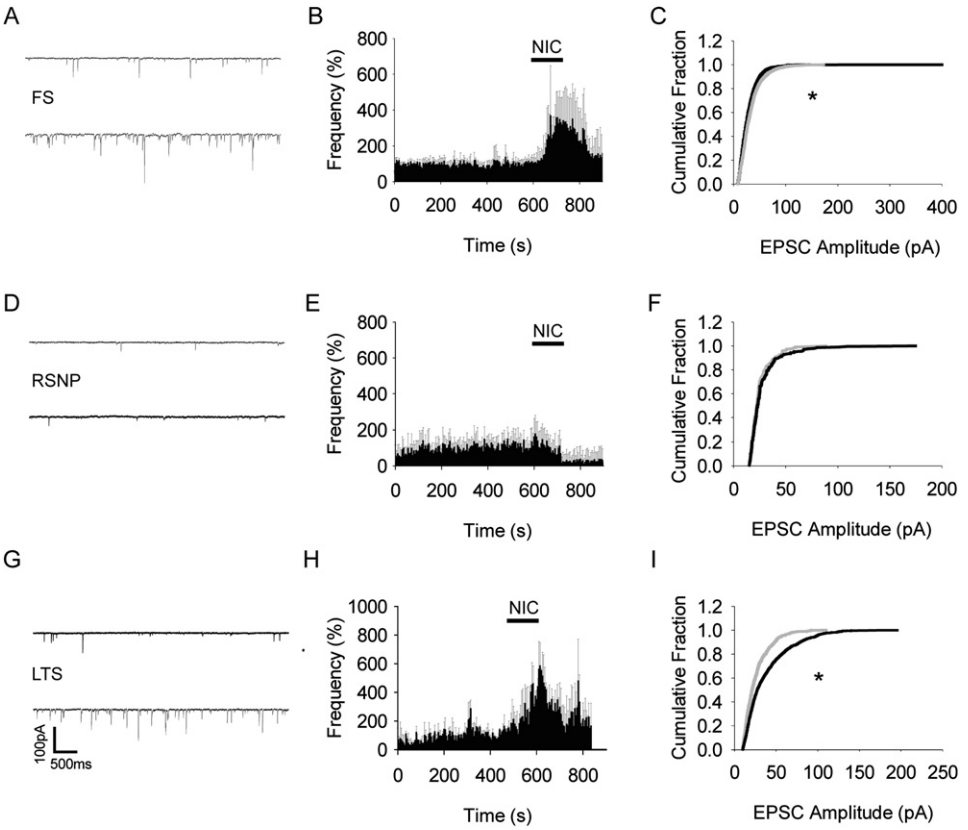

Figure 6. Nicotinic Modulation of Spontaneous EPSCs Received by PFC Interneurons

(A, D, and G) Example EPSC traces recorded from (A) FS, (D) RSNP, and (G) LTS cells, respectively. (B, E, and H) Average EPSC frequency histograms for (B) FS (n = 7); (E) RSNP (n = 11); and (H) LTS cells (n = 3). (C, F, and I) Cumulative amplitude distributions for each of the three cell types are shown. Each graph represents data from the experiments depicted in (A), (D), and (G). *$p < 0.05$. Error bars = SEM.

pyramidal cells are increased in amplitude by nicotine (Figure 4), this could reduce dendritic action potential propagation and subsequent calcium signaling in dendrites of PFC pyramidal neurons.

We first tested whether changes in intracellular calcium concentration are necessary for STDP in mouse PFC layer V pyramidal neurons. When exogenous calcium chelators such as BAPTA are present in the intracellular solution, incoming calcium ions are rapidly buffered and free calcium concentration changes are strongly reduced (Helmchen, 2002; Tsien, 1980). In the presence of BAPTA (10 mM), pairing pre- and postsynaptic activity did not result in an increase of synaptic strength (n = 5, Figures 7A and 7B). Thus, changes in calcium concentration during STDP induction are necessary for changes in synaptic strength to occur.

To investigate whether nicotine reduced calcium transients related to dendritic action potential propagation, we monitored postsynaptic calcium signaling in apical dendrites of layer V pyramidal neurons during timed pre- and postsynaptic activity. Pyramidal neurons were filled with Alexa 594 and the calcium indicator Fluo-4 through patch pipettes and were visualized with two-photon imaging to select a region on the apical dendrite for line-scanning (Figure 7C). As in rat PFC (Gulledge and Stuart, 2003), action potentials invade apical dendrites and induce calcium changes throughout the dendritic tree of mouse pyramidal neurons (Figures 7D–7F). Somatic action potentials were preceded by extracellular stimulation of synaptic input by 5 ms, as was used for the induction of STDP. Line-scans of the apical dendrite were taken 50–100 μm from soma, parallel to the location of extracellular stimulation. After three initial line-scans to obtain baseline measurements, either aCSF or nicotine-containing aCSF was allowed to wash-in for 5 min, after which three line-scans were taken (Figures 7D–7F, right panels). In the presence of nicotine, fluorescence changes of Fluo-4 were reduced by approximately 40% when compared with control conditions in the absence of nicotine (Figures 7E–7G). Thus, in the presence of nicotine, postsynaptic calcium signals associated with coincident pre- and postsynaptic activity were markedly reduced in apical dendrites of PFC pyramidal neurons. In the absence of extracellular stimulation, nicotine did not alter fluorescence changes associated with postsynaptic action potential firing (Figure 7H).This suggests that PFC pyramidal

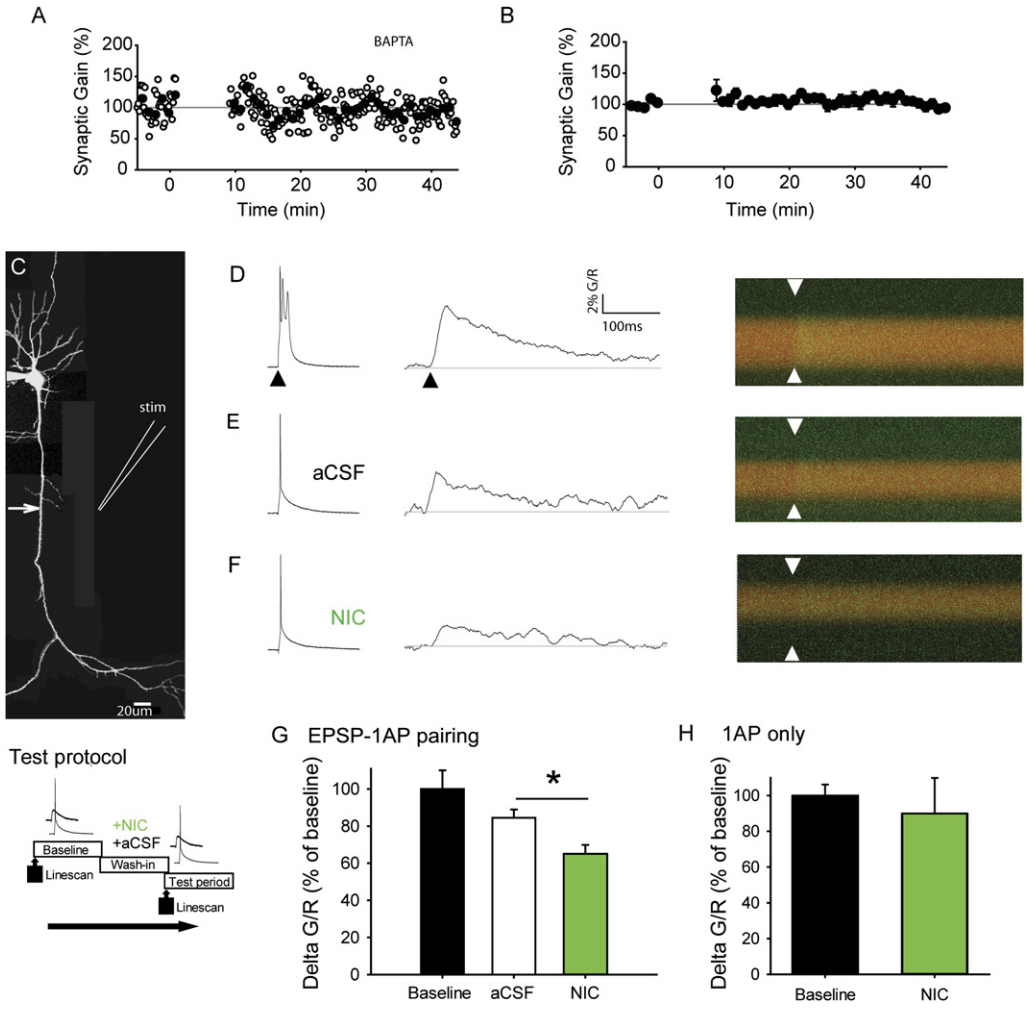

Figure 7. Reduction of AP-Induced Dendritic Calcium Signaling in Nicotine

(A) Example trace showing that STDP is abolished in the presence of 10 mM of the calcium chelator BAPTA.

(B) Summary of effects of BAPTA on STDP (n = 5).

(C) Layer V pyramidal cell filled with Alexa 594, indicating typical position of stimulation electrode and line-scanned ROI (white arrow) Scale bar, 20 μm. (C, Lower panel) Experimental stimulation and line-scan protocol.

(D) Example of calcium transient trace in response to AP burst, showing clear stimulation-induced change in fluorescence across apical dendrite (middle panel).

(E and F) Example traces of single EPSP-AP-induced calcium transients in aCSF (E) and nicotine (F; 10 μM), respectively.

(G) EPSP-AP-induced calcium transients were significantly lower in the presence of nicotine (64% ± 6%, n = 6) compared with aCSF (85% ± 4%, n = 12, *$p < 0.05$).

(H) Nicotine did not induce a significant decrease in AP-induced calcium transients from baseline in the absence of extracellular stimulation (89% ± 20%, n = 3, $p > 0.3$).

Error bars = SEM.

neurons do not express nAChRs that alter dendritic action potential propagation directly. In fact, during application of nicotine in these experiments, the membrane potential of layer V pyramidal neurons did not depolarize, but instead slightly hyperpolarized by –1.7 ± 0.6 mV. In addition, nicotine did not induce changes in baseline fluorescence. In aCSF conditions, baseline fluorescence increased by 3% ± 2%. In the presence of nicotine, baseline fluorescence increased by 4% ± 1.5%, which was not significantly different from aCSF conditions. These data suggest that dendrites of PFC pyramidal neurons do not contain functional nicotinic receptors that directly affect dendritic calcium signaling.

Inhibition of STDP by Nicotine Can Be Overcome by Increased Postsynaptic Activity

Our data suggest that nicotine prevents STDP by decreasing dendritic calcium signaling in pyramidal neurons, not

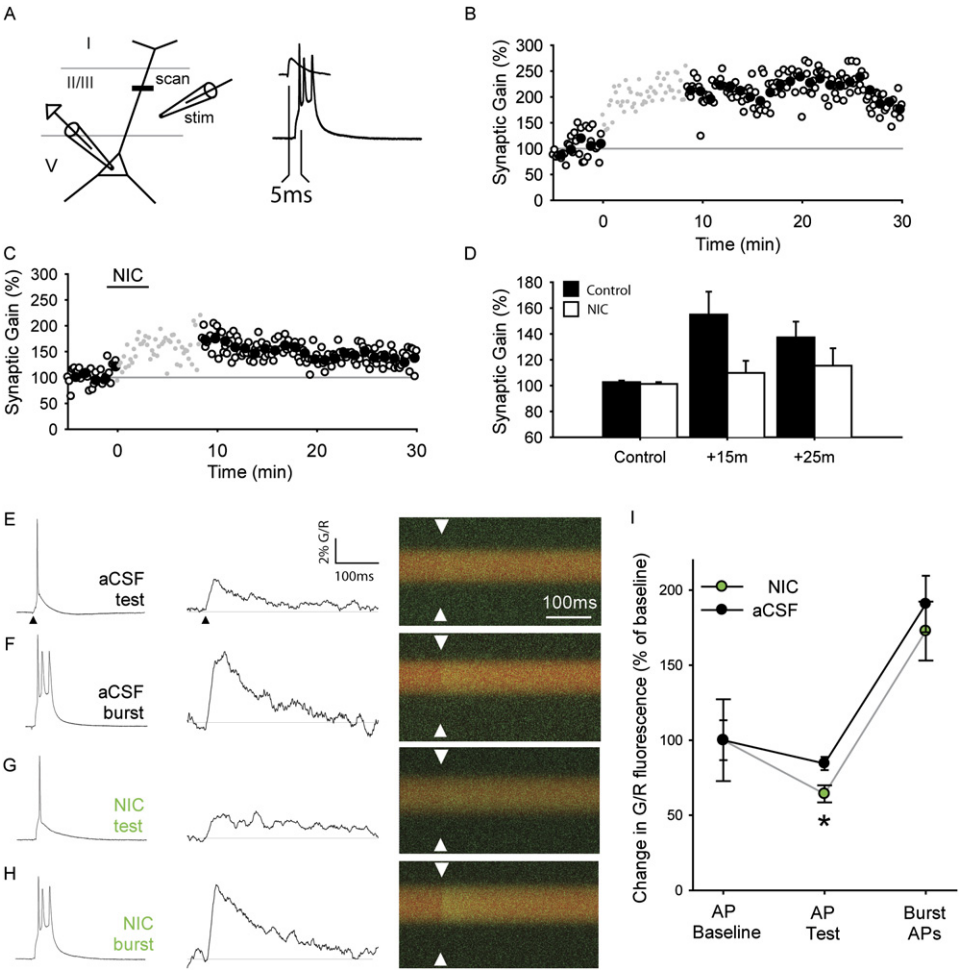

Figure 8. AP Bursts Rescue Nicotine-Impaired Synaptic Plasticity and Increase Calcium Signaling

(A) Diagram of experimental setup. Time delay between EPSP and postsynaptic AP burst of 5 ms during STDP induction is illustrated.

(B and C) Normalized EPSP slope (white circles) and mean slope per minute (black circles) recorded from single experiments in control (B) and nicotine (C).

(D) Summary bar graph of potentiation following EPSP-burst pairing stimulation at 15 min and 25 min after induction.

(E–H) EPSP-AP burst pairings induced significantly larger dendritic calcium transients in layer V pyramidal neurons in both the absence (F) and presence of nicotine (H) than compared with EPSP-single AP pairings in similar conditions (E, G, respectively; aCSF: n = 12 pairwise comparisons, $p < 0.05$; nicotine: n = 6, $p < 0.05$). Arrowheads indicate time point of stimulation.

(I) Nicotine induces a significantly greater decrease in fluorescence following EPSP-single AP pairing compared with aCSF conditions (nicotine: 64% ± 6%, n = 6; aCSF: 85% ± 4%, n = 12, independent samples t test, *$p < 0.05$, data from same experiments as in Figure 7G). Nicotine induces a similar increase in EPSP-AP-burst-induced calcium transients to those in aCSF ($p = 0.5$).

Error bars = SEM.

by reducing the calcium signal directly, but by doing so indirectly by increasing GABAergic inhibition. It follows then that increased postsynaptic action potential firing might overcome the nicotine-induced augmentation of inhibition and block of synaptic potentiation. To test this, we paired single presynaptic events with short bursts of postsynaptic activity with the same delay of 5 ms (Figure 8A). In the absence of nicotine, short bursts of two or three somatic action potentials during a 20 ms depolarization induced an increase in EPSP slope of 151% ± 15% (Figures 8B and 8D). When nicotine was applied during pairing of presynaptic events with postsynaptic bursts, the EPSP slope was still increased (n = 7, Figures 8C and 8D). Thus, the block of STDP by nicotine can be overcome by increased postsynaptic activity, which most likely induces larger calcium changes than a single postsynaptic action potential. To confirm that short bursts of action potentials induce increased postsynaptic calcium signaling in the presence of nicotine, we studied dendritic calcium signaling in response to postsynaptic bursts of action potentials. Short bursts of two or three somatic action potentials during a 20 ms depolarization induced larger changes

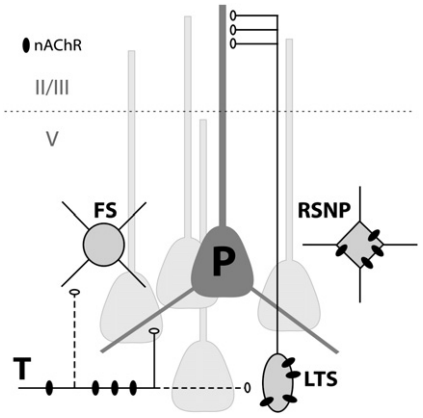

Figure 9. Schematic of the Neuronal Network of Mouse Layer V PFC Depicting the Distribution of nAChRs

P, layer V pyramidal cell; FS, fast-spiking interneuron; RSNP, regular-spiking nonpyramidal neuron; LTS, low-threshold spiking neuron. LTS cells were drawn to synapse on the apical dendrites of pyramidal neurons in line with the description of PFC Martinotti cells provided by Silberberg and Markram (Silberberg and Markram, 2007).

in calcium indicator fluorescence in dendrites than single action potentials (Figures 8E–8I). Bath application of nicotine reduced calcium transients induced by single action potentials, but a short burst of action potentials restored calcium signaling (Figure 8I). These data suggest that spike-timing-dependent plasticity in PFC is blocked by nicotine because calcium signaling during dendritic propagation of single action potentials is altered. This block can be overcome by bursts of action potentials that induce larger calcium signals in dendrites, partially restoring spike-timing-dependent plasticity.

DISCUSSION

Nicotinic receptor stimulation alters PFC-based cognitive performance in primates and rodents (Levin et al., 2005; Levin, 1992; Mansvelder et al., 2006; Newhouse et al., 2004b). In this study, we find that during nAChR activation the timed pairing of presynaptic activity with single postsynaptic action potentials in pyramidal neurons is no longer sufficient to induce LTP of excitatory synapses. Increased postsynaptic activity can overcome this blockade of STDP. During nAChR activation dendritic calcium signaling is reduced, most likely due to increased inhibitory synaptic transmission to pyramidal neurons. Activity of different types of PFC interneurons is increased by nicotine, and we find that different mechanisms are involved (Figure 9). Some interneuron types such as RSNP and LTS cells, express nAChRs somatically. Single-cell PCR data suggest that both cell types express the abundant subunit types $\alpha4$, $\beta2$, and $\alpha7$. FS interneurons do not express nAChRs somatically, but excitatory inputs to these neurons are augmented by nAChR stimulation. Very little mRNA for $\alpha4$, $\beta2$, and $\alpha7$ subunits was found in these cells. Excitatory inputs to LTS cells are also stimulated by nicotine. The net result of these effects is increased GABAergic neurotransmission to pyramidal neurons, reduced dendritic calcium signaling, and an increased threshold for STDP.

Somatic action potentials propagate deep into the dendritic tree and activate voltage-gated calcium channels in proximal and distal parts of dendrites, inducing substantial amounts of calcium influx in dendrites and dendritic spines (Koester and Sakmann, 1998; Stuart et al., 1997; Yuste and Denk, 1995). The control of dendritic action potential propagation, calcium signaling, and spike-timing-dependent plasticity by inhibitory GABAergic transmission has been described in hippocampus (Meredith et al., 2003; Tsubokawa and Ross, 1996). Coincident activation of GABAergic inputs reduced dendritic action potential amplitude and the dendritic calcium signal associated with the action potential (Tsubokawa and Ross, 1996). Pairing of presynaptic activity with single postsynaptic action potentials becomes less effective at potentiating glutamatergic synapses with advancing developmental age. This results from increasing GABAergic inhibition during postnatal development, and can be overcome by pairing presynaptic activity with a burst of several postsynaptic action potentials (Meredith et al., 2003). nAChR stimulation increases GABAergic transmission in hippocampus (Alkondon and Albuquerque, 2001, 2004). Augmentation of GABAergic transmission by nAChR stimulation prevents LTP induced by 100 Hz stimulation for 1 s (Ji et al., 2001). Which postsynaptic mechanisms are involved in this blockade of LTP is not known. In the PFC, we find that with the block of STDP of excitatory transmission, dendritic calcium signaling is strongly reduced when GABAergic transmission is augmented by nicotine. Since transient increases in calcium concentration are fundamental to the induction of LTP (Koester and Sakmann, 1998; Magee and Johnston, 1997; Sjostrom and Nelson, 2002) in PFC pyramidal neurons (Figure 7), this most likely explains why synaptic potentiation fails in the PFC in the presence of nicotine. Thus, stimulation of nAChRs on different types of neurons can change the rules for induction of spike-timing-dependent plasticity in PFC, requiring stronger postsynaptic activity for potentiation to occur.

Nicotine reduced the amount of synaptic potentiation when presynaptic activity was paired to bursts of postsynaptic action potentials. The calcium transients induced by postsynaptic action potential bursts were similar in the presence and absence of nicotine (Figure 8). This suggests that nicotine could be affecting the synaptic plasticity machinery in PFC pyramidal neurons by other mechanisms in addition to reducing calcium signaling. It is well known that in other brain areas, nAChRs are also located on presynaptic neurons that are not glutamatergic or GABAergic, such as dopamine neurons (Wonnacott et al., 2000). It is unknown whether nAChRs are present on any of the monaminergic synapses in the PFC. Dopamine is known to affect synaptic plasticity in PFC (Matsuda et al., 2006; Otani et al., 2003). Nicotinic modulation of dopamine and other monaminergic

neurotransmission in the PFC could contribute to the observed modulation of STDP.

Modification of plasticity rules in cortical neuronal networks by nAChR activation may be a general phenomenon, extending beyond PFC and hippocampus. GABAergic interneurons and inhibitory synaptic transmission are affected by nAChR stimulation in many brain areas (Alkondon and Albuquerque, 2004; Mansvelder et al., 2002, 2006; Metherate, 2004). Just as in hippocampus and PFC, pyramidal neurons in sensory cortical areas are not directly affected by nicotinic agonists, but different types of interneurons are strongly excited by postsynaptic nAChR activation (Alkondon and Albuquerque, 2004; Alkondon et al., 2000; Metherate, 2004; Xiang et al., 1998). Both $\alpha7$ and $\alpha4\beta2$ subunit-containing nAChRs are involved. Many of these interneurons innervate pyramidal neurons, and therefore nAChR-mediated stimulation of interneurons would increase inhibition of pyramidal neurons. Just as we found in PFC pyramidal neurons, this could lead to reduced dendritic action potential propagation and reduced calcium signaling. As a result, stronger postsynaptic activity would be required to overcome this increased dendritic inhibition to induce STDP.

In vivo recordings show that glutamatergic projections between ventral hippocampus and PFC can alter in strength during behavior (Laroche et al., 2000). Projections from the ventral hippocampus CA1 area enter the medial PFC through superficial layers I and II and project to all layers (Jay and Witter, 1991; Laroche et al., 2000). The extent to which synaptic plasticity of these inputs will be affected by nAChR stimulation will most likely depend on the dendritic location of the synapse. Since we found that nAChR stimulation can reduce dendritic calcium signaling associated with postsynaptic action potentials in apical dendrites of layer V pyramidal neurons, it is very likely that plasticity in glutamatergic synapses located distally is most affected by this reduction. At present, it is unknown whether glutamatergic fibers between hippocampus and PFC express nAChRs. Glutamatergic fibers from thalamus that project to PFC layer V pyramidal neurons do express nAChRs and are directly stimulated by nAChR activation (Lambe et al., 2003). These receptors contain $\beta2$ subunits and are most likely not situated on the presynaptic glutamatergic terminals, since the effect of nicotine is mediated by an increase in action potential firing. Projections from the thalamus terminate in deep as well as superficial layers of the rodent medial PFC (Berendse and Groenewegen, 1991; Heidbreder and Groenewegen, 2003). Most likely, synaptic plasticity of thalamocortical terminals synapsing on the distal apical dendrite of layer V pyramidal neurons in superficial layers will suffer more from the nicotinic mechanisms we found to block STDP than the synapses that are located closer to the cell body. By reducing dendritic action potential propagation in apical dendrites, nicotine hampers communication between cell body and distal synapses in layer V pyramidal neurons. This potentially could strongly affect information processing in the neuronal network of the medial PFC as a whole, and will alter the output of the PFC.

The activation of distributed nAChRs provides the PFC neuronal network with a wide range of computational possibilities. Nicotine alters the rules for synaptic plasticity resulting from timed presynaptic and postsynaptic activity by increasing the threshold. Therefore, the function of the medial PFC network will most likely change in the presence of nicotine. Increased activity in pyramidal neurons at least partially restores the conditions needed for STDP to occur. The presence of nicotine and increased threshold for STDP could reduce cognitive performance in healthy, naïve rodents (Day et al., 2006). Alternatively, since PFC neuronal activity could be increased during PFC-based cognitive behavior, nicotine may provide conditions under which signal-to-noise ratio in PFC information processing is enhanced, thereby improving cognitive performance (Day et al., 2006; Mirza and Stolerman, 1998).

EXPERIMENTAL PROCEDURES

Slice Preparation

Prefrontal coronal cortical slices (300 μm) were prepared from P14–23 C57 BL/6 mice, in accordance with Dutch license procedures. Brain slices were prepared in ice-cold artificial cerebrospinal fluid (aCSF), which contained the following: 125 mM NaCl, 3 mM KCl, 1.25 mM NaH_2PO_4, 3 mM $MgSO_4$, 1 mM $CaCl_2$, 26 mM $NaHCO_3$, and 10 mM glucose (300 mOsm). Slices were then transferred to holding chambers in which they were stored in aCSF, which contained the following: 125 mM NaCl, 3 mM KCl, 1.25 mM NaH_2PO_4, 2 mM $MgSO_4$, 1 mM $CaCl_2$, 26 mM $NaHCO_3$, and 10 mM glucose, bubbled with carbogen gas (95% O_2/5% CO_2).

Electrophysiology

Pyramidal cells and interneurons in the medial PFC were first visualized using Hoffman modulation or infrared differential interference contrast microscopy. After the whole-cell configuration was established, recorded responses to steps of current injection allowed us to classify each cell into one of several well-known cortical cell types. In many experiments two-photon imaging was also used to produce an overview of the cell's morphology. All experiments were performed at 31°C–34°C.

Recordings were made using Axopatch or Multiclamp 700A amplifiers (Axon Instruments, CA), sampled at intervals of 50 or 100 μs, digitized by the pClamp software (Axon), and later analyzed off-line (Igor Pro software, Wavemetrics, Lake Oswego, OR). Whole-cell current injection and extracellular stimulation (both timing and levels) were controlled with a Master-8 stimulator (A.M.P.I., Jerusalem, Israel) triggered by the data acquisition software. Patch pipettes (3–5 MOhms) were pulled from standard-wall borosilicate capillaries and were filled with one of three intracellular solutions. For the measurement of EPSCs in pyramidal cells and interneurons, we used a solution containing 140 mM K-gluconate, 1 mM KCl, 10 mM HEPES, 4 mM K-phosphocreatine, 4 mM ATP-Mg, and 0.4 mM GTP (pH 7.2–7.3, pH adjusted to 7.3 with KOH) (290–300 mOsm). The chloride concentration in this intracellular solution was chosen so that the calculated chloride reversal potential was far below the resting membrane potential (−120 mV) and IPSCs would show as outward current in the recording, while EPSCs would show as inward current. This solution was not used in experiments looking specifically at GABAergic activity, where we used an elevated chloride concentration (78 mM potassium gluconate, 70 mM KCl) to make detection of GABA events more reliable. For

the STDP experiments, we used a solution that had a lower osmolarity (110 mM potassium gluconate, 10 mM KCl; 270–275 mOsm) and an elevated phosphocreatine (10 mM) concentration. Series resistance was not compensated.

For the experiments in Figure 2C and Figures 5D–5F, nicotine was applied by pressure ejection from a glass electrode with a tip opening of ~1 μm. Pressure was on for 100 ms. Care was taken that nicotine-containing solution did not leak out of the electrode when no positive pressure was applied by including Alexa 488 (100 μM) in the application pipette so that any leaking solution could be easily visualized using two-photon microscopy. During application, the extent of application was visualized by monitoring the green fluorescence signal of Alexa 488 in some of the experiments.

In the experiments in Figure 3A, we blocked $GABA_A$ receptors to investigate the involvement of GABAergic transmission in the effects of nicotine on STDP. Both bicuculline (1–10 μM) and gabazine (0.25–1 μM) strongly increased the excitability of the PFC network. In some slices, excitation was so strong that spontaneous seizure-like network discharges appeared (Figure S4B). During these discharges, pyramidal neurons received a barrage of synaptic inputs and their membrane potential depolarized by 20–40 mV. In addition, the intracellular calcium concentration in dendrites increased markedly (Figure S4C and S4D). To prevent these bursts from compromising our experiments in any way, we only analyzed experiments during which no network discharges appeared.

Spike-Timing-Dependent Plasticity

EPSPs were evoked every 10 s using an extracellular stimulation electrode positioned in layer II/III (Figure 1A), ~100 μm lateral to the recorded pyramidal cell. The slope of the initial 2.5 ms of the EPSP was analyzed to ensure that the data reflected only the monosynaptic component of each experiment (Froemke et al., 2005). Synaptic gain was measured as the change in average EPSP slope when comparing a 5 min period 20–30 min postconditioning to the baseline EPSP slope measured in the last 5 min of control recording. During the induction protocol spike-timings were measured from the onset of the evoked EPSP to the peak of the postsynaptic action potential. Mean baseline EPSP slopes were averaged from at least 30 sweeps. During the conditioning period presynaptic-postsynaptic stimulus pairing was repeated 50 times, with a 10 s interval between each pairing. An interval between presynaptic stimulation and postsynaptic action potential of 5 ms resulted in reliable potentiation of synaptic strength under control conditions (Figure 1). During experiments cell input resistance was monitored throughout by applying a 10 pA, 500 ms hyperpolarizing pulse at the end of each sweep. Subtle changes in series resistance were usually first detected as a change in the evoked action potential waveform, and experiments were not included in the analysis if the cell input resistance varied by more than ±30% during the experiment. To assess the effect of nicotine in these experiments, nicotine was applied during the induction phase (1 min before through +3 min after start of the 8 min pairing protocol). The Wilcoxon's signed rank test and the Mann-Whitney U-test were used to assess significance. Data are given as mean ± SEM, with $p < 0.05$ indicating significance.

Two-Photon Imaging

Pipettes were tip-filled with intracellular medium and back-filled with intracellular solution containing Alexa 594 (40 μM) to reveal neuronal morphology and the calcium-indicator Fluo-4 (100 or 200 μM, Molecular Probes). Following breakthrough, cells were monitored for a minimum of 15 min to allow diffusion and equilibration of the dye intracellularly before fluorescence measurements were taken. Responses were measured to individual action potentials or two to three action potentials ("burst") during a 20 ms period of current injection. Somatic action potentials were observed during all line-scans analyzed in this data set. To stimulate EPSPs, an extracellular stimulation electrode was placed within 100 μm laterally to the region of apical dendrite being line-scanned in layer II/III. Approximately 5 min after baseline line-scan measurements in aCSF were made, the dendritic region of interest (ROI) was moved ~5 μm closer to the soma, and further line-scans were taken either in aCSF or following bath application of 10 μM nicotine.

A Leica (Mannheim, Germany) RS2 two-photon laser scanning microscope was used with a 63× objective and a Ti:Sapphire laser (Tsunami, SpectraPhysics, CA) tuned to a wavelength of 840 nM for excitation. Line-scan imaging of spines and dendrites was carried out at a temporal resolution of 2 ms/line. Line-scan imaging and electrophysiological recordings were synchronized and all image acquisition was controlled by custom-written macros based on Leica confocal software. Fluorescence was measured across the apical dendrite at a distance of approximately 110 ± 6 μm from the soma. Before stimulation, fluorescence was measured for approx 85 ms to obtain basal fluorescence measurements (Fo). A region of line-scan outside of any indicator-filled ROI was used to measure background fluorescence (Fb). Relative fluorescence changes were calculated as follows: $\Delta G/R=(F(t)-Fo)/(Ro-Rb)$, where Ro is the baseline signal measured with Alexa 594 and Rb is the background signal measured in this channel. $\Delta F/F$ and $\Delta G/R$ signals were measured by detecting the peak change in a trace, averaging a 10 ms region around the peak change, and expressing it as a percentage change from baseline level. Fluorescence traces for single action potentials and bursts of action potentials are averages of three to five traces. Off-line data analysis was carried out using in-house-written procedures in Igor Pro software. Differences between groups were tested using ANOVA and t tests (paired or two-tailed independent samples) in SPSS statistical software, with $p < 0.05$ indicating significance.

Single-Cell Real-Time PCR

For single-cell analyses, we used the same solution as was used for the measurement of spontaneous activity. After recordings were made, the cell was aspirated and the content (~7.5 μl) was expelled in a tube containing 2 μl RT-buffers (final concentrations were 10 mM DTT, 0.5 μM dNTP, and 5 μM random hexamers). An enzyme mixture was added (0.5 μl, containing 50 U MMLV [Promega] and 5 U RNAguard [Amersham]), and after gently mixing, the reaction was performed overnight at 37°C. After precipitation (final concentrations were 2 M NH4Ac, 75% EtOH, and 0.1 μg linear acrylamide) on ice for 30 min, samples were spun (14,000 × g, 30 min), washed twice with 75% EtOH, and collected in 10 μl water. Reactions were stored at 4°C.

For PCR analysis, a preamplification (nAChR subunits, 25 cycles; others, 15 cycles) was followed by amplification (45 cycles) using real-time PCR (10 μl; ABI PRISM 7900, Applied Biosystems). Nested primer sets (see Table S1 in the Supplemental Data) were used for amplification. Whereas the preamplification of GAD, calbindin, CCK, and SOM was carried out in separate reactions (triplicate) using 0.3 μl cDNA, preamplification of the nAChR subunits was performed with a mixture of primers for the α4, α7, and β2 subunits (triplicate) using 1.5 μl cDNA. The amplification was carried out on 2% volume of the preamplification reaction. For each transcript analyzed, a negative control (H_2O) reaction was performed. For both reactions, the SYBR-reagents (2x SYBR-mix; Applied Biosystems) were used, with the following PCR parameters: 10 min at 95°C, followed by 45 cycles using 15 s at 95°C, 1 min at 60°C. For each primer, a positive control (1:10,000 dilution of mouse PFC cDNA) and a negative control (H_2O) were used. At the end of each PCR, a dissociation stage was performed in order to check for specificity of the formed product (from 60°C to 95°C in 15 min; Figure S5). A single PCR round (45 cycles) using β-actin was performed to detect the formation of cDNA, resulting in 52 cells positive out of 54.

Supplemental Data

The Supplemental Data for this article can be found online at http://www.neuron.org/cgi/content/full/54/1/73/DC1/.

ACKNOWLEDGMENTS

We thank Tessa Lodder, Hans Lodder, and Jaap Timmerman for excellent technical support. This work was supported by grants from the Faculty of Earth and Life Sciences and Center of Medical Systems Biology (A.B.S.), the Dutch Medical Research Council (ZonMW 911-03-014 to H.D.M. and A.B.B., and ZonMW 016-076-360 to H.D.M.), and the Royal Netherlands Academy of Arts and Sciences (KNAW, to H.D.M.). Both CNCR departments are financially supported by NeuroBsik (www.neurobsik.nl).

Received: July 13, 2006
Revised: January 22, 2007
Accepted: March 15, 2007
Published: April 4, 2007

REFERENCES

Alkondon, M., and Albuquerque, E.X. (2001). Nicotinic acetylcholine receptor alpha7 and alpha4beta2 subtypes differentially control GABAergic input to CA1 neurons in rat hippocampus. J. Neurophysiol. *86*, 3043–3055.

Alkondon, M., and Albuquerque, E.X. (2004). The nicotinic acetylcholine receptor subtypes and their function in the hippocampus and cerebral cortex. Prog. Brain Res. *145*, 109–120.

Alkondon, M., Pereira, E.F., Eisenberg, H.M., and Albuquerque, E.X. (2000). Nicotinic receptor activation in human cerebral cortical interneurons: a mechanism for inhibition and disinhibition of neuronal networks. J. Neurosci. *20*, 66–75.

Berendse, H.W., and Groenewegen, H.J. (1991). Restricted cortical termination fields of the midline and intralaminar thalamic nuclei in the rat. Neuroscience *42*, 73–102.

Bi, G.Q., and Poo, M.M. (1998). Synaptic modifications in cultured hippocampal neurons: dependence on spike timing, synaptic strength, and postsynaptic cell type. J. Neurosci. *18*, 10464–10472.

Cauli, B., Porter, J.T., Tsuzuki, K., Lambolez, B., Rossier, J., Quenet, B., and Audinat, E. (2000). Classification of fusiform neocortical interneurons based on unsupervised clustering. Proc. Natl. Acad. Sci. USA *97*, 6144–6149.

Dalley, J.W., Cardinal, R.N., and Robbins, T.W. (2004). Prefrontal executive and cognitive functions in rodents: neural and neurochemical substrates. Neurosci. Biobehav. Rev. *28*, 771–784.

Dani, J.A., and Harris, R.A. (2005). Nicotine addiction and comorbidity with alcohol abuse and mental illness. Nat. Neurosci. *8*, 1465–1470.

Day, M., Pan, J.B., Buckley, M.J., Cronin, E., Hollingsworth, P.R., Hirst, W.D., Navarra, R., Sullivan, J.P., Decker, M.W., and Fox, G.B. (2006). Differential effects of ciproxifan and nicotine on impulsivity and attention measures in the 5-choice serial reaction time test. Biochem. Pharmacol., in press.

Froemke, R.C., Poo, M.M., and Dan, Y. (2005). Spike-timing-dependent synaptic plasticity depends on dendritic location. Nature *434*, 221–225.

Gabbott, P.L., Dickie, B.G., Vaid, R.R., Headlam, A.J., and Bacon, S.J. (1997). Local-circuit neurones in the medial prefrontal cortex (areas *25*, 32 and 24b) in the rat: morphology and quantitative distribution. J. Comp. Neurol. *377*, 465–499.

Ge, S., and Dani, J.A. (2005). Nicotinic acetylcholine receptors at glutamate synapses facilitate long-term depression or potentiation. J. Neurosci. *25*, 6084–6091.

Gioanni, Y., Rougeot, C., Clarke, P.B., Lepouse, C., Thierry, A.M., and Vidal, C. (1999). Nicotinic receptors in the rat prefrontal cortex: increase in glutamate release and facilitation of mediodorsal thalamocortical transmission. Eur. J. Neurosci. *11*, 18–30.

Granon, S., Poucet, B., Thinus-Blanc, C., Changeux, J.P., and Vidal, C. (1995). Nicotinic and muscarinic receptors in the rat prefrontal cortex: differential roles in working memory, response selection and effortful processing. Psychopharmacology (Berl.) *119*, 139–144.

Gray, R., Rajan, A.S., Radcliffe, K.A., Yakehiro, M., and Dani, J.A. (1996). Hippocampal synaptic transmission enhanced by low concentrations of nicotine. Nature *383*, 713–716.

Groenewegen, H.J., and Uylings, H.B. (2000). The prefrontal cortex and the integration of sensory, limbic and autonomic information. Prog. Brain Res. *126*, 3–28.

Gulledge, A.T., and Stuart, G.J. (2003). Action potential initiation and propagation in layer 5 pyramidal neurons of the rat prefrontal cortex: absence of dopamine modulation. J. Neurosci. *23*, 11363–11372.

Gulledge, A.T., Park, S.B., Kawaguchi, Y., and Stuart, G.J. (2007). Heterogeneity of phasic cholinergic signaling in neocortical neurons. J. Neurophysiol. *97*, 2215–2229. Published online November 22, 2006. 10.1152/jn.00493.2006.

Heidbreder, C.A., and Groenewegen, H.J. (2003). The medial prefrontal cortex in the rat: evidence for a dorso-ventral distinction based upon functional and anatomical characteristics. Neurosci. Biobehav. Rev. *27*, 555–579.

Helmchen, F. (2002). Raising the speed limit - fast Ca(2+) handling in dendritic spines. Trends Neurosci. *25*, 438–441.

Henningfield, J.E., Stapleton, J.M., Benowitz, N.L., Grayson, R.F., and London, E.D. (1993). Higher levels of nicotine in arterial than in venous blood after cigarette smoking. Drug Alcohol Depend. *33*, 23–29.

Jay, T.M., and Witter, M.P. (1991). Distribution of hippocampal CA1 and subicular efferents in the prefrontal cortex of the rat studied by means of anterograde transport of Phaseolus vulgaris-leucoagglutinin. J. Comp. Neurol. *313*, 574–586.

Jay, T.M., Burette, F., and Laroche, S. (1995). NMDA receptor-dependent long-term potentiation in the hippocampal afferent fibre system to the prefrontal cortex in the rat. Eur. J. Neurosci. *7*, 247–250.

Ji, D., Lape, R., and Dani, J.A. (2001). Timing and location of nicotinic activity enhances or depresses hippocampal synaptic plasticity. Neuron *31*, 131–141.

Kawaguchi, Y. (1993). Groupings of nonpyramidal and pyramidal cells with specific physiological and morphological characteristics in rat frontal cortex. J. Neurophysiol. *69*, 416–431.

Kawaguchi, Y., and Kondo, S. (2002). Parvalbumin, somatostatin and cholecystokinin as chemical markers for specific GABAergic interneuron types in the rat frontal cortex. J. Neurocytol. *31*, 277–287.

Kawaguchi, Y., and Kubota, Y. (1997). GABAergic cell subtypes and their synaptic connections in rat frontal cortex. Cereb. Cortex *7*, 476–486.

Koester, H.J., and Sakmann, B. (1998). Calcium dynamics in single spines during coincident pre- and postsynaptic activity depend on relative timing of back-propagating action potentials and subthreshold excitatory postsynaptic potentials. Proc. Natl. Acad. Sci. USA *95*, 9596–9601.

Lambe, E.K., Picciotto, M.R., and Aghajanian, G.K. (2003). Nicotine Induces Glutamate Release from Thalamocortical Terminals in Prefrontal Cortex. Neuropsychopharmacology *28*, 216–225.

Laroche, S., Jay, T.M., and Thierry, A.-M. (1990). Long-term potentiation in the prefrontal cortex following stimulation of the hippocampal CA1/subicular region. Neurosci. Lett. *114*, 184–190.

Laroche, S., Davis, S., and Jay, T.M. (2000). Plasticity at hippocampal to prefrontal cortex synapses: dual roles in working memory and consolidation. Hippocampus *10*, 438–446.

Levin, E., McClernon, F., and Rezvani, A. (2005). Nicotinic effects on cognitive function: behavioral characterization, pharmacological specification, and anatomic localization. Psychopharmacology (Berl.)

184, 523–539. Published online October 12, 2005. 10.1007/s00213-005-0164-7.

Levin, E.D. (1992). Nicotinic systems and cognitive function. Psychopharmacology (Berl.) *108*, 417–431.

Liss, B. (2002). Improved quantitative real-time RT-PCR for expression profiling of individual cells. Nucleic Acids Res. *30*, e89.

MacDermott, A.B., Role, L.W., and Siegelbaum, S.A. (1999). Presynaptic ionotropic receptors and the control of transmitter release. Annu. Rev. Neurosci. *22*, 443–485.

Magee, J.C., and Johnston, D. (1997). A synaptically controlled, associative signal for Hebbian plasticity in hippocampal neurons. Science *275*, 209–213.

Malenka, R.C., Kauer, J.A., Zucker, R.S., and Nicoll, R.A. (1988). Postsynaptic calcium is sufficient for potentiation of hippocampal synaptic transmission. Science *242*, 81–84.

Mansvelder, H.D., and McGehee, D.S. (2000). Long-term potentiation of excitatory inputs to brain reward areas by nicotine. Neuron *27*, 349–357.

Mansvelder, H.D., and McGehee, D.S. (2002). Cellular and synaptic mechanisms of nicotine addiction. J. Neurobiol. *53*, 606–617.

Mansvelder, H.D., Keath, J.R., and McGehee, D.S. (2002). Synaptic mechanisms underlie nicotine-induced excitability of brain reward areas. Neuron *33*, 905–919.

Mansvelder, H.D., van Aerde, K., Couey, J., and Brussaard, A. (2006). Nicotinic modulation of neuronal networks: from receptors to cognition. Psychopharmacology (Berl.) *184*, 292–305.

Markram, H., Lubke, J., Frotscher, M., and Sakmann, B. (1997). Regulation of synaptic efficacy by coincidence of postsynaptic APs and EPSPs. Science *275*, 213–215.

Matsuda, Y., Marzo, A., and Otani, S. (2006). The presence of background dopamine signal converts long-term synaptic depression to potentiation in rat prefrontal cortex. J. Neurosci. *26*, 4803–4810.

McGehee, D.S., and Role, L.W. (1995). Physiological diversity of nicotinic acetylcholine receptors expressed by vertebrate neurons. Annu. Rev. Physiol. *57*, 521–546.

McGehee, D.S., and Role, L.W. (1996). Presynaptic ionotropic receptors. Curr. Opin. Neurobiol. *6*, 342–349.

McGehee, D.S., Heath, M.J., Gelber, S., Devay, P., and Role, L.W. (1995). Nicotine enhancement of fast excitatory synaptic transmission in CNS by presynaptic receptors. Science *269*, 1692–1696.

Meredith, R.M., Floyer-Lea, A.M., and Paulsen, O. (2003). Maturation of long-term potentiation induction rules in rodent hippocampus: role of GABAergic inhibition. J. Neurosci. *23*, 11142–11146.

Metherate, R. (2004). Nicotinic acetylcholine receptors in sensory cortex. Learn. Mem. *11*, 50–59.

Mirza, N.R., and Stolerman, I.P. (1998). Nicotine enhances sustained attention in the rat under specific task conditions. Psychopharmacology (Berl.) *138*, 266–274.

Muir, J.L., Everitt, B.J., and Robbins, T.W. (1995). Reversal of visual attentional dysfunction following lesions of the cholinergic basal forebrain by physostigmine and nicotine but not by the 5-HT3 receptor antagonist, ondansetron. Psychopharmacology (Berl.) *118*, 82–92.

Newhouse, P., Singh, A., and Potter, A. (2004a). Nicotine and nicotinic receptor involvement in neuropsychiatric disorders. Curr. Top. Med. Chem. *4*, 267–282.

Newhouse, P.A., Potter, A., and Singh, A. (2004b). Effects of nicotinic stimulation on cognitive performance. Curr. Opin. Pharmacol. *4*, 36–46.

Otani, S., Daniel, H., Roisin, M.P., and Crepel, F. (2003). Dopaminergic modulation of long-term synaptic plasticity in rat prefrontal neurons. Cereb. Cortex *13*, 1251–1256.

Picciotto, M.R., and Zoli, M. (2002). Nicotinic receptors in aging and dementia. J. Neurobiol. *53*, 641–655.

Silberberg, G., and Markram, H. (2007). Disynaptic inhibition between neocortical pyramidal cells mediated by Martinotti cells. Neuron *53*, 735–746.

Sjostrom, P.J., and Nelson, S.B. (2002). Spike timing, calcium signals and synaptic plasticity. Curr. Opin. Neurobiol. *12*, 305–314.

Stuart, G., Spruston, N., Sakmann, B., and Hausser, M. (1997). Action potential initiation and backpropagation in neurons of the mammalian CNS. Trends Neurosci. *20*, 125–131.

Tsien, R.Y. (1980). New calcium indicators and buffers with high selectivity against magnesium and protons: design, synthesis, and properties of prototype structures. Biochemistry *19*, 2396–2404.

Tsubokawa, H., and Ross, W.N. (1996). IPSPs modulate spike backpropagation and associated [Ca2+]i changes in the dendrites of hippocampal CA1 pyramidal neurons. J. Neurophysiol. *76*, 2896–2906.

Vidal, C., and Changeux, J.P. (1989). Pharmacological profile of nicotinic acetylcholine receptors in the rat prefrontal cortex: an electrophysiological study in a slice preparation. Neuroscience *29*, 261–270.

Vidal, C., and Changeux, J.P. (1993). Nicotinic and muscarinic modulations of excitatory synaptic transmission in the rat prefrontal cortex in vitro. Neuroscience *56*, 23–32.

Wonnacott, S., Kaiser, S., Mogg, A., Soliakov, L., and Jones, I.W. (2000). Presynaptic nicotinic receptors modulating dopamine release in the rat striatum. Eur. J. Pharmacol. *393*, 51–58.

Wonnacott, S., Sidhpura, N., and Balfour, D.J. (2005). Nicotine: from molecular mechanisms to behaviour. Curr. Opin. Pharmacol. *5*, 53–59.

Xiang, Z., Huguenard, J.R., and Prince, D.A. (1998). Cholinergic switching within neocortical inhibitory networks. Science *281*, 985–988.

Yang, C.R., Seamans, J.K., and Gorelova, N. (1996). Electrophysiological and morphological properties of layers V-VI principal pyramidal cells in rat prefrontal cortex in vitro. J. Neurosci. *16*, 1904–1921.

Yuste, R., and Denk, W. (1995). Dendritic spines as basic functional units of neuronal integration. Nature *375*, 682–684.